ELSEVIER

Cell Biology International 27 (2003) 921–928

Cell Biology International

www.elsevier.com/locate/cellbi

Comparative NMR studies of diffusional water permeability of red blood cells from different species: XIV. Little Penguin, *Eudyptula minor*

G.H. Benga[1]*, B.E. Chapman[2], G.C. Cox[3], P.W. Kuchel[2]

[1] *Department of Cell and Molecular Biology, "Iuliu Hatieganu" University of Medicine and Pharmacy, 6 Pasteur St, 3400, Cluj-Napoca, Romania*
[2] *School of Molecular and Microbial Biosciences, University of Sydney, NSW, Australia*
[3] *The Australian Key Center for Microscopy and Microanalysis, University of Sydney, NSW, Australia*

Received 10 October 2002; revised 2 June 2003; accepted 9 July 2003

Abstract

As part of a programme of comparative measurements of diffusional water permeability (P_d) the red blood cells (RBC) from Little Penguin (*Eudyptula minor*) were studied. The cell dimensions were measured with light and electron microscopy, and by a newly described non-invasive technique, NMR *q*-space analysis. In view of its relative novelty for cell biologists, an overview of this technique is presented. The RBC revealed an ellipsoidal shape that is characteristic of avian RBC, with axis lengths ("diameters") estimated to be: a=16.0 μm; b=9.6 μm; c=5.0 μm. The values of P_d were: 2.0×10^{-3} cm s^{-1} at 5 °C, 3.3×10^{-3} cm s^{-1} at 10 °C, 4.6×10^{-3}cm s^{-1} at 15 °C and $\sim 5.4 \times 10^{-3}$ cm s^{-1} at 20, 25, 30, 37 and 42 °C.

There was a lack of inhibition of water permeability by *p*-chloromercuribenzensulfonate (PCMBS), the well-known inhibitor of RBC aquaporin. It was notable that in the temperature range 5–20 °C the NMR parameters, and hence the permeability, varied linearly as is found for other species, but at temperatures higher than 20 °C there was no temperature-dependence of P_d. Consequently, there was an obvious break at ~20 °C in the Arrhenius plot, of the mean residence life time of water inside the cells, $1/T_e$, versus temperature. For temperatures less than 20 °C the activation energy $E_{a,d}$ was 45.6 ± 6.6 kJ/mol. For temperatures higher than 25 °C $E_{a,d}$ was zero. The lack of inhibition of water permeability by PCMBS and the very high value of $E_{a,d}$ for diffusive water exchange suggests that the water permeation occurs primarily via the membrane bilayer per se, i.e., there is no aquaporin in Little Penguin RBC. The discontinuity at ~20 °C in the Arrhenius plot is an interesting finding, not seen before in other species, and we suggest that it reflects a phase transition in the membrane lipids.

Keywords: NMR; Water permeability; Aquaporin; Red blood cells; Little Penguin

1. Introduction

All living cells (except for some spores) are filled with water and surrounded by a plasma membrane, whose main property is semi- or selective permeability to water and solutes. In fact, the concept of a functional plasma membrane enclosing the cell contents emerged from permeability studies (see reviews by Benga, 1988, 1989; Macey, 1984). Simple lipid bilayers exhibit water permeability, and yet membranes of, for example, red blood cells (RBC), that contain space-occluding proteins, are also very permeable to water. Thus, Macey and Farmer (1970), amongst others, have postulated that this water exchange takes place via selective proteinaceous channels; this hypothesis was realized in the late 1980s and early 1990s, when a family of water-exchanging proteins (called aquaporins) were identified throughout nature.

Rapid advances in the understanding of the structure and mechanism of water channel proteins have occurred since the first evidence for such a protein in human RBC (Benga et al., 1986a,b) and its isolation and characterization by Agre and coworkers a few years later (Preston et al., 1992). The name change from CHIP28 to the now generally accepted aquaporin 1 (AQP1) took

* Corresponding author. Tel.: +40-64-194373; fax: +40-64-197257
E-mail address: gbenga@personal.ro (G.H. Benga).

1065-6995/03/$ - see front matter
doi:10.1016/j.cellbi.2003.07.005

place as the wide distribution of such proteins across all phyla was realized. The three-dimensional structure of aquaporin 1 at 3.8 Å resolution has recently been described (Murata et al., 2000).

Despite these important advances in understanding the structural determinants of water permeation through aquaporins, their physiological role in the RBC membrane is still not fully understood. Investigations of RBC from various species could help shed light on the physiological significance of this transport process, since correlations between water permeability and other characteristics of RBC, or of the whole organism, could be established. As part of a programme of comparative measurements of diffusional water permeability, the RBC from selected laboratory, domestic and wild animals have been investigated (Benga et al., 1993a,b,c,d,e; Benga et al., 1994a,b, 1995, 1996, 1999, 2000a,b, 2002).

We report here the first nuclear magnetic resonance (NMR) measurements of the diffusional water permeability, P_d, of RBC from Little Penguin (*Eudyptula minor*). This bird is interesting in the present context because it spends a large part of its life in seawater. The measurement of P_d requires an estimate of cell dimensions and volume, and hence a calculation of the surface area of the cell membrane. The cell dimensions were measured with light and electron microscopy, and by a newly described non-invasive technique, NMR *q*-space analysis. In addition to membrane water permeability, the activation energy of the permeation was measured. Also, in view of its relative novelty for cell biologists, an overview of NMR *q*-space analysis for measuring cell sizes is given.

Because of its unique habitat, and in order to set the present analysis in the broader context of the lifestyle of this bird, we give the following background information. The Little Penguin is the smallest of all penguins. It is also called the Fairy or Blue Penguin, and is the only one to breed in Australia and the only one to wait until dark before coming ashore to roost. Leaving the surf, they form groups and cross the beach to sand dunes and cliffs, where they roost in crevices and burrows excavated under tussocks (del Hoyo et al., 1992). The evening return of ~1000 birds to a protected area of dunes at Summerlands Beach, Philip Island, Victoria is a famous tourist attraction (Pizzey, 1991). Penguins are the most maritime of all birds, being recognized by three main features: modification of wings into flippers, upright stance on land, and strongly counter-shaded plumage (Pizzey, 1991). The Little Penguin feeds on small fish, squid and crustaceans, it captures prey by means of pursuit-diving, and is known to dive down to 69 m (Blakers et al., 1984).

The Little Penguin's habitat is the temperate marine waters of islands and coastal waters of Southern Australia, from Freemantle to Northern New South Wales, Tasmania, Bass Strait islands and New Zealand, including Stewart and Chatham islands (Blakers et al., 1984; del Hoyo et al., 1992; Pizzey, 1991). Although not globally threatened, there are under 1 million birds in Australia. Generally, wherever human habitation has encroached on, and radically altered, breeding grounds, populations have declined or disappeared (Blakers et al., 1984). Hence, a better understanding of all physiological characteristics of this species is desirable, particularly an understanding of how it adapted to temperate maritime waters, when all other species of penguin live in much colder waters.

2. Theory of *q*-space measurements

This experiment entails measuring the intensity (area of the peak) of the water signal from the sample, as a function of the magnitude of the magnetic field gradient pulses, g, used in the pulsed field-gradient spin-echo (PGSE) experiment (e.g., Kuchel et al., 1997). The experiment was carried out with fixed values of pulse duration, δ and time interval between them, $\mathbf{\Delta q}$ is a scaled form of $\mathbf{g}$ and is given by $\mathbf{q}=(2\pi)^{-1}\,\gamma\,\mathbf{g}\delta$, where γ is the magnetogyric ratio of the nucleus under investigation, in the present case ^{1}H in water, $\mathbf{q}$ is a vector (same direction as $\mathbf{g}$) with units of m^{-1} and as such it is referred to as a 'spatial wave number vector' with its reciprocal denoting a distance.

When a *q*-space experiment is conducted on a sample that contains no barriers to water (apart from the walls of the NMR tube) the plot declines as a monotonically strictly decreasing function that has the shape of a half-Gaussian curve (Kuchel et al., 1997). If there are barriers to water diffusion on a micrometre distance-scale, with a narrow distribution of separations (such as exists in a suspension of RBC), then the curve displays a series of peaks and troughs or 'coherence' features. These features arise from water molecules diffusing in the restricting spaces outside the cells, and from water undergoing restricted diffusion inside the cells. The former effect has been called "pore-hopping" (Callaghan et al., 1991) and it yields a coherence pattern that is the counterpart of the two- or multiple-slit interference effect of physical optics. Diffusion inside the cells yields a signal-coherence effect that is the counterpart of single-slit diffraction; hence it is called 'diffusion-diffraction'.

As in physical optics, there is a simple relationship between the position of the coherence maxima or minima and the separation between the barriers; in the case of diffusion-coherence it is the distance between the barriers (that limit the translational motion of the diffusing molecules) that is the counterpart of the slit in optics. However, if there is variation in cell size, as is seen with human red cells that undergo crenation, the *q*-space plot loses its coherence "wiggles". In this situation, an estimate of the mean cell dimensions can still

be obtained as follows: the *q*-space data are Fourier transformed and the resulting Gaussian curve is used to obtain its width-at-half-height ($\Delta_{1/2}$). This value is related to the root-mean-square separation (Δz_{rms}) between the diffusion barriers, in this case the cell membranes by the expression:

$$\Delta z_{rms} = \Delta_{1/2}/(2[2 \ln 2]^{1/2}) \quad (1)$$

An interesting outcome from adding diamagnetic (CO-treated) RBC into the intense magnetic field, $\mathbf{B}_0$, of an NMR spectrometer is that the cells align with the field with their axis of rotational symmetry perpendicular to $\mathbf{B}_0$. In the present series of experiments, diffusion was measured in the direction of this main magnetic field so the characteristic distance that was measured was a diameter of the (aligned) RBC. When studying ellipsoidal RBC, such as those from birds, it is not obvious whether the alignment will be with the main/maximum diameter or the intermediate one, or some average of these; this matter is discussed below.

In recent work is has been shown that for *q*-space plots the coherence peaks predicted for water undergoing "pore-hopping"/interference outside human RBC in a high-haematocrit, ~75% suspension, are much less intense than the diffusion-diffraction coherence peaks from water diffusing inside the RBC. Since the first diffusion-interference peak and the first diffusion-diffraction peak overlap, and the second diffusion-interference peak is of low intensity, it is the position of the second diffusion-diffraction minimum that yields the most reliable estimate of the diameter of the RBC (Torres et al., 1999). Thus, the RBC diameter is given by an empirical factor, divided by the value of $q_{min,2}$; the empirical factor of 2.82 was obtained from data generated by computer simulation of water diffusion in an array of discocytes and it is close to the value of 2.46, derived analytically for a sphere (Torres et al., 1999).

3. Materials and methods

3.1. RBC

Samples of Little Penguin (*E. minor*) blood were obtained from Taronga Zoo, Sydney, NSW, Australia. Blood samples were collected into heparin (15 IU/ml), refrigerated within 30 min and used within 72 h. RBC were isolated by centrifugation, washed three times in medium S: 150 mM NaCl, 5.5 mM glucose, 5 mM HEPES [4-(2-hydroxyethyl)-1-piperazine ethanesulfonic acid], pH 7.4, and suspended at a haematocrit of 30–40% in the same solution supplemented with 0.5% (w/v) bovine serum albumin. The incubation of RBC with 0.4 mM *p*-(chloromercuri) benzenesulfonate (PCMBS) was performed on washed RBC (suspended in medium S at a haematocrit of 10%) for 60 min at 37 °C. After incubation, the erythrocytes were washed three times in medium S, and each washing was followed by centrifugation to remove the reagent. Finally, RBC were suspended in medium S supplemented with 0.5% bovine serum albumin at a haematocrit of 50%.

3.2. NMR equipment

The NMR experiments were carried out on a Bruker DRX 400 NMR spectrometer operating at 400.13 MHz for ^{1}H detection, with an Oxford Instruments wide-bore 9.4 T magnet. The spectrometer was equipped for diffusion measurements with a power-supply and probe that delivered magnetic field-gradient pulses up to a maximum of 10 T m^{-1}, in the direction of the main magnetic field, $\mathbf{B}_0$.

3.3. q-*Space experiments*

For these, the RBC were washed twice (2000 × *g*, 10 min, 5 °C) in saline solution (154 mM NaCl) containing 10 mM glucose, with the buffy coat being removed after the first centrifugation step. The cell suspension was bubbled with CO to convert the haemoglobin to the stable diamagnetic form that ensures a narrow NMR signal from the water in the sample (Kuchel et al., 1997). After a third wash, 0.5 ml of the sample of haematocrit 35–75% was added to an 8 mm external diameter flat-bottomed glass NMR tube (Wilmad, Buena, NJ, USA). A Teflon vortex plug was inserted into the tube and pushed down on to the meniscus; excess RBC suspension was removed to leave a sample height of 1 cm. Then the flat-bottomed tube was inserted into a 10 mm outer-diameter NMR tube to which had been added neat CCl_4. The latter compound has a magnetic susceptibility that is close to those of the RBC suspension and glass, thus obviating magnetic field inhomogeneities at the interfaces between the sample, the glass and air.

The standard pulsed field-gradient spin-echo (PFGSE) pulse sequence and phase cycles were used (Kuchel et al., 1997; Torres et al., 1998, 1999). The probe temperature was set to 25 °C. The duration of the $\pi/2$ pulse was 22 μs; that of the two gradient pulses, δ, was 2 ms; the time interval between the gradient pulses was 20 ms; the relaxation delay between transients was 3 s; and the number of transients per spectrum was 32. The field gradient was incremented in steps of 2% of the maximum attainable value and after 50 steps the value was 9.9 T m^{-1}.

The acquired data consisted of 1 k of complex points spanning a spectral width of 1 kHz. There was no zero-filling of the data, and a line-broadening factor of 5 Hz was used with exponential multiplication of the data prior to its Fourier transformation. A *Mathematica* program was used to process and analyse the data as *q*-space plots and their Fourier transformations.

3.4. P_d measurements

The water diffusion exchange time (T_e) was measured by the Mn^{2+}-doping ^1H NMR method (Conlon and Outhred, 1972; Morariu and Benga, 1977) on the Bruker DRX 400 wb NMR spectrometer (see above) as previously described (Benga et al., 1993b,c, 1994a,b).

The transverse relaxation time of the water in the cell interior (T_{2i}) was measured on packed cells (haematocrit 95%), from which the supernatant with no added Mn^{2+} had been removed by centrifugation. Samples for NMR measurements of the water proton relaxation time T'_{2a} (the prime denotes the fact that this is a composite relaxation time) were prepared by gentle mixing of 0.4 ml RBC suspended in medium S (haematocrit 30–40%) and 0.2 ml doping solution (40 mM $MnCl_2$, 100 mM NaCl). As shown by Conlon and Outhred (1972), T'_{2a} and T_{2i} are parameters that are required to estimate the water diffusion exchange time (T_e), by using the equation:

$$1/T_e = 1/T'_{2a} - 1/T_{2i} \quad (2)$$

The membrane permeability for water diffusion, P_d, is related to $1/T_e$ by the expression involving the cell water volume (V) and the cell surface area (A):

$$P_d = (1/T_e)\,(V/A) \quad (3)$$

Other details of the measurement of water permeability and activation energy of this transport process were carried out as previously described (Benga et al., 1987, 1990a,b).

3.5. Morphological measurements with microscopy

The mean cell volume was calculated from measurements of haematocrit and mean cell count using either a Sysmex-CC 130 Microcell counter (Tao Medical Electronics Co. Ltd, Kobe, Japan) or a Thoma counting chamber; the latter was used to avoid errors in the electronic counter due to variations in cell sizes (Jain, 1986). All such measurements were performed on four samples of the same blood.

The cell water content was determined by drying samples of RBC to constant weight (15 h at 110 °C) and calculating water volume as a fraction of cell volume, as described by Savitz et al. (1964). The fractional volume of water in Little Penguin RBC was 0.7.

The surface area of the ellipsoidal cells was calculated from the diameters based on equations described by Bulliman and Kuchel (1988) and Jensen and Brahm (1995). In addition, the cell surface areas were calculated from the mean cell diameters when the cells were swollen to spheres in hypotonic NaCl solution containing 0.5% (w/v) albumin and 1 mm PCMBS. The measurements were performed by light microscopy using an image analyser (Tracor Northern TN 8507, Madison, WI, USA) as described by Benga et al. (1993b). The diameters were measured in two ways: with cells photographed in a light microscope or in a scanning electron microscope. The measurements were performed only on cells lying completely flat or exactly on edge. For scanning electron microscopy, samples of pelleted washed RBC were prepared as described by Benga et al. (1996), examined and photographed in a Jeol JSM-6300 F scanning electron microscope. Human RBC with a diameter of 8 μm was taken as a reference (Benga et al., 1993a).

4. Results

4.1. Morphology

The light micrograph (Fig. 1A) and scanning electron micrograph (Fig. 1B) of penguin RBC are presented here for the first time and they show the well-known ellipsoidal shape that is characteristic of avian RBC. The excellent resolution of the micrographs made it possible to measure accurately the axis lengths ("diameters") of the RBC. A correction was carried out for diameters measured on electron micrographs as previously described (Benga et al., 1993a). The diameters were estimated to be: a=16.00 ± 0.90 μm; b=9.38 ± 0.47 μm; c=4.95 ± 0.27 μm (mean ± SD) for 65 cells.

4.2. q-Space data

Fig. 2A shows a q-space plot obtained from a sample of RBC from Little Penguin. It is clear that the coherence pattern is not as well delineated as that routinely observed with human and other mammalian RBC (Torres et al., 1998, 1999; Benga et al., 2000a). The fact that avian RBC are ellipsoidal alone would not account for this outcome; but the fact that they contain a central nucleus and may have a more heterogeneous size distribution would account for a loss of definition of the coherence features in the plot. Nevertheless, it was possible to discern positions of local minima in the plot, and these are indicated by arrows in Fig. 2A. They occur at $q = 1.44 \times 10^5$, 2.84×10^5, and 4.56×10^5 m^{-1}, respectively. For biconcave discs, the diameter of the discocyte is given by $\alpha_i/q_{min.i}$, where i is the order of the minimum, and α is equal to 1.43, 2.82, and 4.19, respectively (Regan and Kuchel, 2002).

The first two better-defined minima each give a value of 9.93 μm for the main diameter of the cells. To convey a sense of the uncertainty in these estimates, we consider those that arise from using the q-values at each point on either side of the first two minima; the values are (in μm) 11.11 and 8.84, and 10.49 and 9.40, respectively. The mean and standard deviation of all six values is 9.95 ± 0.80 μm. We stress that this is a very conservative

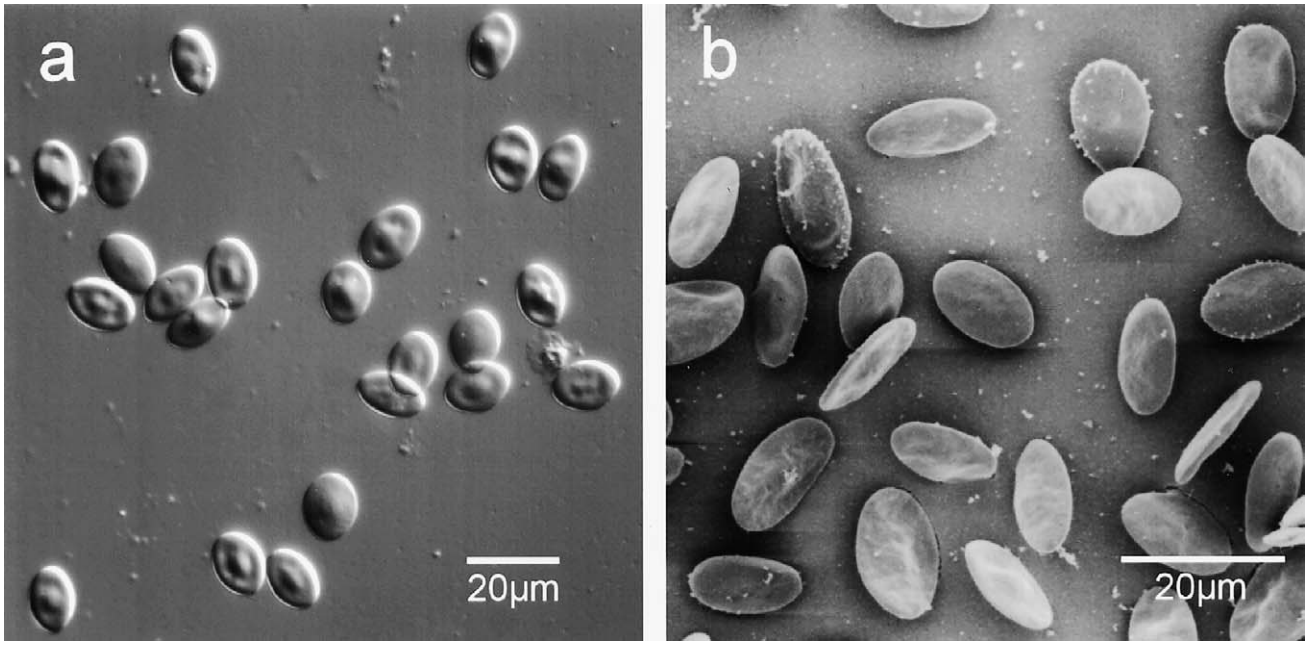

Fig. 1. Morphology of Little Penguin RBC. (a) light micrograph: images were recorded using a 40 × 0.75 n.a. DIC objective. (b) electron micrograph. Details of sample preparation are indicated in Materials and methods.

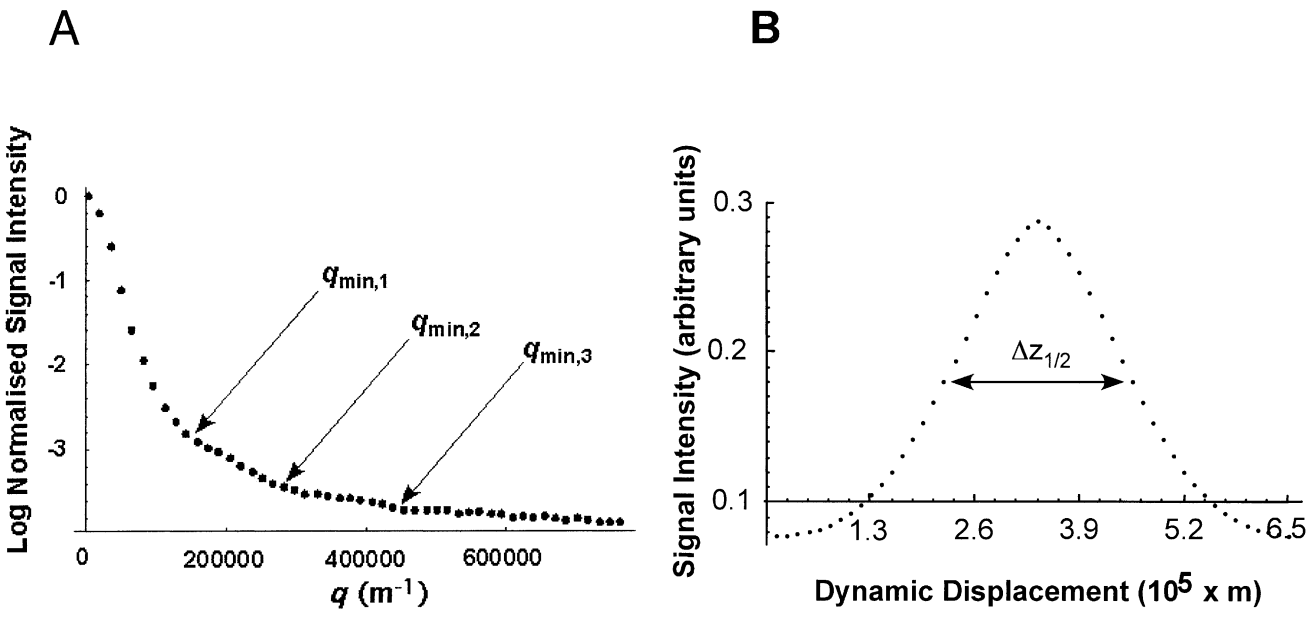

Fig. 2. q-Space determination of the mean diameter of RBC from Little Penguin. (A) ^{1}H NMR q-space plot of water in a 35% haematocrit suspension of fresh RBC, at 25 °C. The spin-echo signal intensity was normalized and graphed using the Log_{10} values. The abscissa location of apparent inflection points are denoted $q_{\mathrm{min},1-3}$. The (minor) coherence features of the curves are primarily due to intracellular diffusion-diffraction of water (Torres et al., 1999); and the q-positions of the diffraction minima are inversely related to the mean cell diameter, bearing in mind that the cells are aligned with their longest axis parallel to the magnetic field in the NMR spectrometer magnet (Kuchel et al., 1997). (B) Fourier transformation of the data in A, used to reveal the form of the so-called diffusion propagator, which is apparently Gaussian; its width-at-half-height, $\Delta z_{1/2}$, yields the mean separation between the diffusion-restricting barriers, which are the cell membranes.

estimate of the standard deviation and a simple way to refine the value is to reduce the steps in q-values used in the experiment. Halving these values yields a mean and standard deviation of 9.93 ± 0.40 μm. Further discussion of error analysis of q-space data is given in Torres et al. (1999).

Fourier transformation of the data, and rescaling the abscissa to reflect displacement, yielded Fig. 2B. The

Table 1
Parameters characterizing water diffusional permeability of RBC from Little Penguin

No. of determinations (no. of animals)	Temperature of measurement (°C)	T'_{2a} (ms)	T_e (ms)	P_d ($10^3 \times$ cm s^{-1})
6 (6)	5	17.3 ± 2.7	36.7 ± 11.5	2.0 ± 0.5
6 (6)	10	13.5 ± 1.9	22.2 ± 4.8	3.3 ± 0.7
6 (6)	15	11.0 ± 1.7	15.9 ± 3.5	4.6 ± 1.0
6 (6)	20	9.8 ± 1.5	13.6 ± 2.9	5.4 ± 1.1
14 (8)	25	9.3 ± 1.3	13.2 ± 2.2	5.4 ± 0.9
8 (7)	30	9.3 ± 1.4	13.2 ± 2.5	5.6 ± 0.9
11 (8)	37	10.1 ± 0.7	14.0 ± 1.3	5.0 ± 0.5
6 (6)	42	9.8 ± 1.0	13.2 ± 1.8	5.4 ± 0.9

For details of preparation, measurements and calculations see Materials and methods. The values are means ± SD. Under the same experimental conditions, the average values (10^3 cm s^{-1}) of P_d of human RBC for three healthy donors were: 4.4 at 25 °C; 5.5 at 30 °C; 6.5 at 37 °C; and 7.8 at 42 °C.

rescaling used the fact derived from Fourier theory that the interval between points in dynamic-displacement space is equal to the reciprocal of the maximum value of q used in the experiment, denoted here as q_{max}. Hence the maximum value of the dynamic displacement represented on the abscissa in Fig. 2B is the number of points, 50, multiplied by $1/q_{max}$, which yielded 6.5×10^{-5} m. The width-at-half-height of the peak above the zero-baseline in Fig. 2B is encompassed by 16 points, and using Eq. (1) this yielded an RMS displacement (i.e. cell diameter projected in the direction of the main magnetic field) of 8.9 μm. With respect to the present data, this form of analysis appears to be quite robust, as the main diameter measured for the cells was within 1 μm by both methods of analysis. Although this value equates moderately well with the intermediate-axis value of the cells measured by light microscopy, the fact that it is the intermediate value and not the maximum one begs further discussion (see below).

4.3. Estimates of P_d

The NMR parameters and the diffusional water permeability (P_d) of penguin RBC are listed in Table 1. There was also a lack of inhibition of water permeability by PCMBS, carried out under the conditions described in Materials and methods and as used in our previous studies on RBC from other animals.

It was notable that NMR parameters, and hence permeability, varied linearly, as expected, in the temperature range 5–20 °C, but at temperatures higher than 20 °C there was no temperature-dependence of P_d. In other words, there is an obvious break at ~20 °C in the Arrhenius plot of the mean residence life time of water inside the cells, $1/T_e$, versus temperature (Fig. 3). Consequently, two values of the activation energy of water diffusion were calculated on the basis of this plot, one for temperatures below, and the other for temperatures above, 20 °C. For temperatures less than 20 °C the activation energy was 45.6 ± 6.6 kJ/mol (mean ± SD for six determinations on RBC from six animals). For temperatures higher than 25 °C, the activation energy was zero.

5. Discussion

5.1. q-Space analysis

An advantage of the new q-space analysis for measuring the dimensions of cells is that the cells require: (1) no pre-treatment, (2) they experience minimal contact with glass surfaces that can, in the case of RBC, precipitate echinocyte formation, and (3) the method is non-invasive, so the cells can be used for other analyses, such as measuring their metabolic or membrane transport characteristics. However, a limitation of the method is that a direct analysis of the q-space plot using the reciprocal of positions of minima requires the sample to have a very narrow size and shape distribution. Thus, the plots of our samples of penguin RBC showed less-pronounced diffusion-diffraction features than RBC from the other species studied thus far.

It is possible to enhance the features of q-space plots by using numerical differentiation of the data. However, this introduces noise, and in our experience it does not

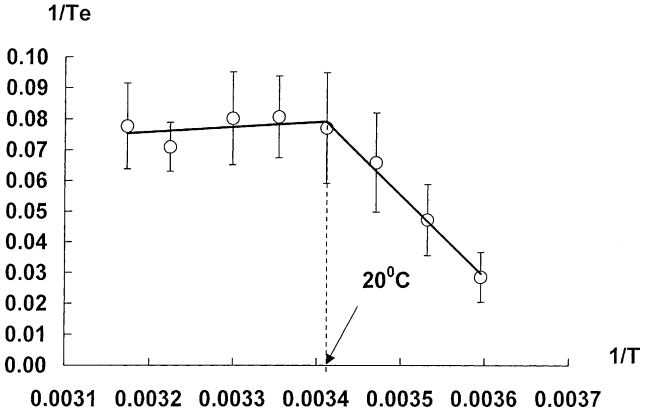

Fig. 3. Arrhenius plot of the water exchange time in penguin RBC.

greatly improve the ability to perceive the positions of inflections in the plots. On the other hand, when the plot is smooth and virtually Gaussian in shape, Fourier transformation of the data yields a Gaussian-shaped single peak; its width-at-half-height can be measured with good precision, but the location of the baseline can be problematical. In this study, it was taken to be the zero value. Thus, via Eq. (1), it yields an estimate of the inter-barrier distance for the restricted diffusion of water in the sample. Under the experimental conditions (long diffusion time of 40 ms) used here, this value was that of the apparent mean cell-diameter.

It is now well-established that oxygenated and carbon monoxygenated human RBC that have the shape of biconcave discs become aligned with their disc-planes parallel to the $\mathbf{B}_0$ field in an NMR spectrometer. The physical basis of the alignment is that the hydrocarbon chains of the phospholipids have diamagnetic anisotropy and their minimum energy orientation is across the magnetic field. Therefore, when phospholipids are in a membrane, its preferred orientation is with its surface parallel to the field. On the other hand, it can be shown from classical magnetostatics that both dia- and paramagnetic disc-shaped bodies (such as RBC) have a minimum energy orientation that is perpendicular to the field.

Thus, there is 'competition' between the membrane-diamagnetic-anisotropy effect and the 'dia- or paramagnetic body' effect, for the orientation. In the case of oxygenated human RBC, the membrane effects "wins". However, what is the situation in this orientation "contest" with a flattened ellipsoid? Until the present work, it was not known if the cells would be aligned in the magnetic field with their maximum or intermediate axis in the direction of $\mathbf{B}_0$ (with the flat surfaces still parallel to $\mathbf{B}_0$ in the latter case). The value, 9.9 μm, matches the intermediate axis-length measured using optical and electron microscopy.

The effect of the interaction of the flattened elongated (ellipsoidal) diamagnetic-body with $\mathbf{B}_0$ is to maximize the length of the body across $\mathbf{B}_0$. The effect of the membrane diamagnetic anisotropy is to maximize the number of hydrocarbon chains in the membrane lying across $\mathbf{B}_0$; in other words with the flat surface parallel to $\mathbf{B}_0$. A physical "compromise" is to have the flat faces of the ellipsoid parallel to $\mathbf{B}_0$ but the long axis of the ellipsoid across the field. Therefore, the value of the ellipsoid diameter that is projected in the direction of $\mathbf{B}_0$, and which is measured in the q-space analysis, is the intermediate diameter.

5.2. RBC water permeability

It has previously been shown in chicken RBC that the permeation of water through membrane proteins plays no major role, since P_d is much lower than that of mammalian RBC, and is not affected by PCMBS. Also, the permeability has a relatively high E_{ad} value, which is characteristic of simple lipid-bilayer membranes (Benga et al., 1996).

The lack of inhibition of water permeability of penguin RBC by PCMBS and the very high value of E_{ad} suggests that water permeation occurs primarily via the membrane bilayer. The discontinuity in the Arrhenius plot at $\sim$20 °C is an interesting finding that has not been seen before in any other species. It may be that it reflects a phase transition of the membrane lipids. Such a phase transition has been postulated for human RBC membranes (Zimmer and Schirmer, 1974), although this has remained a controversial issue (Morariu et al., 1981). It is possible that, in the case of penguin RBC, such a lipid phase transition does occur. If so, how does this correlate with the functional characteristics of this species? This matter deserves further investigation. This makes further comparative studies of the membrane water permeability in RBC from different avian species relevant to a molecular understanding of water diffusion across red cell membranes.

Acknowledgements

We thank Dr William Bubb and Mr William Lowe (School of Molecular and Microbial Biosciences, University of Sydney), Dr Ed Lonnon (Taronga Zoo, Sydney), Dr Horea Matei, Adrian Florea and Eugen Mironescu (Department of Cell and Molecular Biology, "Iuliu HaTieganu" University of Medicine and Pharmacy Cluj-Napoca) for assistance with the experimental, secretarial and computer work, and to the National Council for Higher Education Scientific Research of Romania (grant 219) for financial support.

References

Benga Gh. Water transport in red blood cell membrane. Prog Mol Biol 1988;51:193–245.

Benga Gh. Water exchange through the erythrocyte membrane. Int Rev Cytol 1989;114:273–316.

Benga Gh, Popescu O, Borza V, Pop VI, Mureşan A, Mocsy I et al. Water permeability of human erythrocytes. Identification of membrane proteins involved in water transport. Eur J Cell Biol 1986a; 41:252–62.

Benga Gh, Popescu O, Pop VI, Holmes PR. p-(Chloromercuri) benzenesulfonate binding by membrane proteins and the inhibition of water transport in human erythrocytes. Biochemistry 1986b; 25:1535–8.

Benga Gh, Pop VI, Popescu O, Hodârnău A, Borza V, Presecan E. Effects of temperature on water diffusion in human erythrocytes and ghosts—nuclear magnetic resonance studies. Biochim Biophys Acta 1987;905:339–48.

Benga Gh, Pop VI, Popescu O, Borza V. On measuring the diffusional water permeability of human red blood cells and ghosts by nuclear magnetic resonance. J Biochem Biophys Methods 1990a;21: 87–102.

Benga Gh, Popescu O, Borza V, Pop VI, Wrigglesworth JM. Water transport in human red cells: effects of non-inhibitory sulphydryl reagents on membrane proteins and water exchange. Rev Roum Biochim 1990b;27:189–98.

Benga Gh, Borza T, Popescu O, Poruţiu D, Matei H. Comparative nuclear magnetic resonance studies of diffusional water permeability of red blood cells from sheep and cow. Comp Biochem Physiol 1993a;104B:589–94.

Benga Gh, Chapman BE, Gallagher CH, Agar N, Kuchel P. NMR studies on diffusional water permeability from eight species of marsupial. Comp Biochem Physiol 1993b;106A:515–8.

Benga Gh, Chapman BE, Coopers D, Kuchel PW. NMR studies on diffusional water permeability studies of red blood cells from Macropodid marsupials (Kangaroos and Wallabies). Comp Biochem Physiol 1993c;104A:799–803.

Benga Gh, Matei H, Borza T, Poruţiu D, Lupşe C. Comparative nuclear magnetic resonance studies on water diffusional permeability of red blood cells from mice and rats. Comp Biochem Physiol 1993d;104A:491–5.

Benga Gh, Matei H, Borza T, Poruţiu D, Lupşe C. Comparative nuclear magnetic resonance studies of diffusional water permeability of red blood cells from differential species. V-Rabbit (Oryctolagus cuniculus). Comp Biochem Physiol 1993e;106B: 281–5.

Benga Gh, Chapman BE, Hinds L, Huchel PW. Comparative NMR studies of diffusional water permeability of erythrocytes from some animals introduced to Australia: rat, rabbit and sheep. Comp Haematol Int 1994a;4:232–5.

Benga Gh, Ralston GB, Borza T, Chapman BE, Gallagher CH, Kuchel PW. NMR studies of diffusional water permeability of red blood cells from Echidna (Tachyloglossus aculeatus). Comp Biochem Physiol 1994b;107B:45–50.

Benga Gh, Borza T, Matei H, Hodor P, Frenţescu L, Ghiran I et al. Comparative nuclear magnetic resonance studies of diffusional water permeability of red blood cells from different species. VIII. Adult and fetal guinea pig (Cavia porcellus). Comp Haematol Int 1995;5:106–11.

Benga Gh, Matei H, Chapman BE, Bulliman BT, Gallagher CH, Agar NS et al. Comparative nuclear magnetic resonance studies of diffusional water permeability of red blood cells from different species. IX. Australian feral chicken and domestic chicken (Gallus domesticus). Comp Haematol Int 1996;6:92–5.

Benga Gh, Grieve SM, Chapman BE, Gallagher CH, Kuchel PW. Comparative NMR studies of diffusional water permeability of red blood cells from different species X. Camel (Camelus dromedarius) and alpaca (Lama pacos). Comp Haematol Int 1999;9:43–8.

Benga Gh, Kuchel PW, Chapman BE, Cox GC, Ghiran I, Gallagher CH. Comparative cell shape and diffusional water permeability of red blood cells from Indian elephant (Elephas maximus) and man (Homo sapiens). Comp Haematol Int 2000a;10:1–8.

Benga Gh, Matei H, Frenţescu L, Kuchel PW, Chapman BE, Cox GC et al. Comparative nuclear magnetic resonance studies of diffusional water cells from different species. XI. Horses introduced to Australia and European horses. Comp Haematol Int 2000b; 10:138–43.

Benga Gh, Ghiran I, Matei H, Frenţescu L, Florea A. Comparative nuclear magnetic resonance studies of diffusional water permeability of red blood cells from different species. XII Dog (Canis familiaris) and cat (Felis domestica). Comp Clin Path 2002; 11:1–10.

Blakers M, Davies SJJF, Reilly PN.. The atlas of Australian birds. Melbourne (Australia): University Press, 1984;7–8.

Bulliman BT, Kuchel PW. Aseries expression for the surface area of an ellipsoid and its application to the computation of the surface area of avian erythrocytes. J Theor Biol 1988;134:113–23.

Callaghan PT, Coy A, McGowan D, Pacher KJ, Zelaya FO. Diffraction-like effects in NMRT diffusion studies of fluids in porous solids. Nature 1991;351:457–69.

Conlon T, Outhred R. Water diffusion permeability of erythrocytes using an NMR technique. Biochim Biophys Acta 1972;288:354–61.

del Hoyo J, Elliot A, Sargatal J, editors. Handbook of the birds of the world. Barcelona: Lynx. Edicions, 1992;914.

Jensen FB, Brahm J. Kinetics of chloride transport across fish red blood cell membranes. J Comp Biol 1995;198:2237–44.

Jain NC. Schalm's veterinary hematology, 4th edn Philadelphia: Lea and Febiger, 1986.

Kuchel PW, Coy A, Stilbs P. NMR "diffusion-diffraction" of water revealing alignment of erythrocytes in a magnetic field and their dimensions and membrane transport characteristics. Magn Reson Med 1997;3:637–43.

Macey RI. Transport of water and urea in red blood cells. Am J Physiol 1984;246:195–203.

Macey RI, Farmer REL. Inhibition of water and solute permeability in human red cells. Biochim Biophys Acta 1970;211:104–6.

Morariu VV, Benga Gh. Evaluation of a nuclear magnetic resonance technique for the study of water exchange through erythrocyte membranes in normal and pathological subjects. Biochim Biophys Acta 1977;469:301–10.

Morariu V, Pop VI, Popescu O, Benga Gh. Effects of temperature and pH on the water exchange through erythrocyte membranes: nuclear magnetic resonance studies. J Membr Biol 1981;62:1–5.

Murata K, Mitsuoka K, Hirai T, Walz T, Agre P, Heymann VB et al. Structural determinants of water permeation through aquaporin-1. Nature 2000;407:599–605.

Pizzey G, Robertson A, editors. A field guide to the birds of Australia 1991;28–9.

Preston GM, Caroll TP, Guggino WB, Agre P. Appearance of water channels in Xenopus oocytes expressing red cell CHIP28 protein. Science 1992;256:365–87.

Regan DG, Kuchel PW. Simulation of molecular diffusion in lattices of cells: insights for NMR of red blood cells. Biophys J 2002; 83:161–71.

Savitz D, Sidel VW, Solomon AK. Osmotic properties of human red cells. J Gen Physiol 1964;48:79–94.

Torres AM, Michniewicz RJ, Chapman BE, Young GAR, Kuchel PW. Characterization of erythrocyte shapes and size by NMR diffusion-diffraction of water: correlations with electron micrographs. Magn Reson Imaging 1998;16:423–34.

Torres AM, Taurins AT, Regan DG, Chapman BE, Kuchel PW. Assignment of coherence features in NMR q-space plots to particular diffusion modes in erythrocyte suspensions. J Magn Reson 1999;138:135–43.

Zimmer G, Schirmer H. Viscosity change of erythrocyte membranes and membrane lipids at transition temperature. Biochim Biophys Acta 1974;345:314–21.